Computational studies of heterogeneous reactions of SiH2 on reconstructed Si(111)–(7×7) and Si(111)–(1×1) surfaces

Paras M. Agrawal, Donald L. Thompson, and Lionel M. Raff

Citation: The Journal of Chemical Physics **91**, 5021 (1989); doi: 10.1063/1.457618
View online: http://dx.doi.org/10.1063/1.457618
View Table of Contents: http://scitation.aip.org/content/aip/journal/jcp/91/8?ver=pdfcov
Published by the AIP Publishing

Computational studies of heterogeneous reactions of SiH_2 on reconstructed Si(111)–(7×7) and Si(111)–(1×1) surfaces

Paras M. Agrawal, Donald L. Thompson, and Lionel M. Raff
Department of Chemistry, Oklahoma State University, Stillwater, Oklahoma 74078

(Received 15 February 1989; accepted 11 July 1989)

The dynamics of chemisorption and decomposition of SiH_2 on Si(111)–(1×1) and recontructed Si(111)–(7×7) surfaces have been investigated using classical trajectories on a previously described [Surf. Sci. **195**, 283 (1988)] potential-energy surface modified to yield the experimental bending frequencies for chemisorbed hydrogen atoms and to incorporate the results of *ab initio* calculations of the repulsive interaction between SiH_2 and closed-shell lattice atoms. The Binnig *et al.* model is employed for the (7×7) reconstruction. Sticking probabilities are found to be unity on the (1×1) surface and near unity on Si(111)–(7×7). The major mode of surface decomposition on the (7×7) surface is by direct molecular elimination of H_2 into the gas phase. Hydrogen atom dissociation to adjacent lattice sites is a much slower process and the chemisorbed hydrogen atoms thus formed exhibit very short lifetimes on the order of $(1.13–10.6)\times10^{-13}$ s. The calculated rate coefficients for these two decomposition modes are 3.4×10^{10} and 0.79×10^{10} s^{-1}, respectively. The rate coefficients for the corresponding reactions on the (1×1) surface are 6.6×10^{10} and 5.3×10^{10} s^{-1}, respectively. The rates on the (1×1) surface are faster due to the increased exothermicity released by the formation of two tetrahedral Si–Si bonds upon chemisorption compared to a single Si–Si bond on the (7×7) surface. Molecular beam deposition/decomposition experiments of SiH_4 on Si(111)–(7×7) surfaces reported by Farnaam and Olander [Surf. Sci. **145**, 390 (1984)] indicate that chemisorbed hydrogen atoms are not formed in the SiH_4 decomposition process whereas the present calculations suggest that such a reaction, although slow, does occur subsequent to SiH_2 chemisorption. It is suggested that energetic differences between SiH_4 and SiH_2 chemisorption are responsible for these differences.

I. INTRODUCTION

Heterogeneous reactions of SiH_2 on Si(111) surfaces constitute some of the most fundamental processes involved in the chemical vapor deposition (CVD) of silicon from silane. Jasinski *et al.*[1] and Bloem *et al.*[2] have published extensive reviews of silicon CVD. We have recently reported the results of a theoretical study of the dynamics of chemisorption and reaction of SiH_2 on the Si(111)–(1×1) surface.[3] [Hereafter, we will refer to this as paper I] In this investigation, we found the SiH_2 sticking probabilities to be unity for all temperatures and incident translational energies studied. Chemisorption results in a tetrahedrally bonded structure to two adjacent lattice sites with the exothermicity of chemisorption being primarily dissipated into the phonon modes of the lattice. Decomposition on the surface occurs via two modes: direct molecular hydrogen elimination and a two-step sequence in which successive hydrogen atoms dissociate to surface binding sites in a plane perpendicular to the *–Si–* plane. Direct hydrogen atom abstraction by the surface prior to chemisorption was not observed. The first-order rate coefficients for the elementary surface reactions show the sequential dissociation of hydrogen atoms to the lattice to be the major decomposition mode.

The above results are in qualitative accord with the model proposed by Robertson and Gallagher[4] for SiH_4 surface reaction. Their mechanism consists of a series of 14 elementary steps in which dissociation of hydrogen atoms to surface adsorption sites plays a key role. However, recent experimental evidence obtained by Farnaam and Olander[5] on thermal cracking of silane on Si(111) suggests a very different reaction mechanism. Simultaneous surface reaction of SiH_4 and SiD_4 shows that only H_2 and D_2 are produced in the gas phase. No isotopic mixing is observed, suggesting the absence of hydrogen and deuterium atoms on the surface. Consequently, Farnaam and Olander[5] suggest that silane reaction on Si(111) involves the formation of two bound SiH_2 molecules upon chemisorption of SiH_4. These two SiH_2 molecules are presumably bound in different types of adsorption sites and decompose to $Si + H_2$.

While our previous theoretical studies[3] show that direct desorption of H_2 into the gas phase is an important SiH_2 decomposition path, the major reaction mode is dissociation of hydrogen atoms to the surface. This lack of agreement with the data reported by Farnaam and Olander[5] may be due to several factors that include (a) inaccuracies in the empirical potential-energy surface used to describe the SiH_2–Si(111)–(1×1) interaction, and (b) differences in the reaction mechanisms for thermal cracking of SiH_4 and direct chemisorption of SiH_2.

Our previous studies of silicon surface reactions of SiH_2 employed a three-layer model of the Si(111)–(1×1) surface. At temperatures of interest in silicon CVD, however, it is expected that reconstruction will occur leading to a (7×7) structure. Such a (7×7) reconstruction of silicon is well established[6] and several experimental studies of heterogeneous reactions of different gaseous systems on this sur-

 0021-9606/89/205021-09$02.10

face have been reported.[1,5–16] Binnig *et al.*[17] have used scanning tunneling microscopy (STM) to characterize the Si(111)–(7×7) reconstruction. They noted that the STM images of Si(111)–(7×7) are characterized by 12 protrusions (interpreted as adatoms) and by a deep corner hole. Based on these observations, Binnig *et al.*[17] proposed the modified adatom model shown in Fig. 1. This model has a (7×7) unit cell with 12 adatoms with dangling bonds in the top layer (A). These 12 adatoms are bonded to 36 atoms in the second layer (B). Each unit cell contains 25 atoms with dangling bonds, 12 and 13 in layers A and B, respectively. The absence of the adatom at the corner of the unit cell is clearly seen in Fig. 1. Tromp[18] and Yamaguchi[19] have investigated changes in the surface topology of this model by considering substrate relaxation.

Using data obtained from ultrahigh vacuum transmission electron diffraction and microscopy, Takayanagai *et al.*[20,21] have proposed another model of the Si(111)–(7×7) reconstruction called the DAS model (dimer–adatom–stacking fault). In this model, there are 19 silicon atoms with dangling bonds per unit cell, 12 in layer A, 6 in layer B, and one in the fourth layer (D). The number of dangling bonds for this model is the lowest among all of the proposed models for the (7×7) reconstruction.[17,22–31] Tromp and van Loenen[32] have recently reviewed various models of Si(111)–(7×7).

In the present paper, we present the results of a theoretical investigation of the heterogeneous processes of chemisorption and reaction of SiH_2 on Si(111)–(7×7) using the lattice model proposed by Binnig *et al.*[17] The choice of the Binnig model simplifies the computational problems by eliminating the necessity of treating a silicon atom with a dangling bond in the fourth layer, as proposed by the DAS model. The presence of such an atom would require the inclusion of fifth layer atoms in the calculations which would probably increase the accuracy required for the interaction parameters between SiH_2 and the third and fourth layer atoms of the lattice. Since the 12 adatoms of layer A and the relative positions of the silicon atoms with dangling bonds in layer B and the nearest adatom of layer A are the same in both the unrelaxed DAS and Binnig models, the results may well be insensitive to the choice of models. This point will be investigated in subsequent studies.

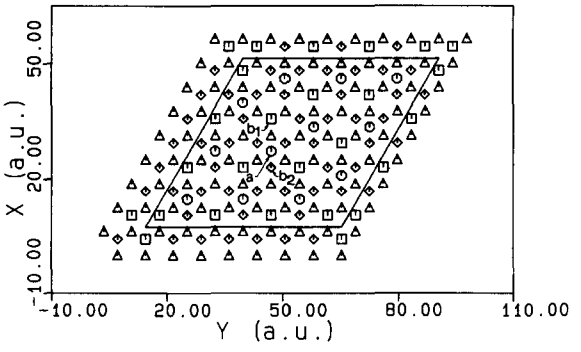

FIG. 1. *X*–*Y* coordinates of the lattice atoms in the unrelaxed state for the (7×7) reconstruction given by Binnig *et al.* Octagonals denote the 12 atoms of the top layer, squares represent the 26 atoms of layer B with dangling bonds, rotated squares show the second layer closed-shell silicon atoms, and triangles specify the third layer atoms. The parallelogram bounds a unit cell of the lattice.

In the following section, we describe the lattice model in more detail. The potential-energy surface is given in Sec. III. Section IV reports the results. The major finding of the study is that on the (7×7) reconstruction, the major SiH_2 decomposition pathway is direct elimination of H_2 into the gas phase. Dissociation of hydrogen atoms to adjacent surface sites is a slow process and the chemisorbed hydrogen atoms formed in the reaction have a very short lifetime.

II. LATTICE MODEL

In paper I,[3] we have used a 95-atom lattice model for the Si(111)–(1×1) surface. Of these 95 atoms, 25 top-layer atoms have dangling bonds. The second and third layers each contain 35 atoms. The motion of the 25 top-layer atoms is explicitly considered in the calculations while the remaining 70 atoms are considered frozen in their equilibrium positions. The results obtained from this lattice model have been summarized in the previous section.

For the (7×7) reconstruction, we have utilized the structure proposed by Binnig *et al.*[17] To minimize the effect of the finite size of the unit cell, the 32 atoms surrounding the 49 atoms of the unit cell in layer B have also been included in the model as shown in Fig. 1. Thus, our lattice model contains the 12 adatoms found by Binnig *et al.*[17] in layer A, 81 silicon atoms in layer B, 99 in layer C, and 99 in layer D, giving a total of 291 atoms. The use of 99 atoms in layer C against 81 in B allows each of the 81 atoms of B to form three bonds with layer C. If layers B and C are modeled with an equal number of atoms, the peripheral atoms of B will not be completely bound by layer C with the result that the computed strain energy may be too small. For example, Yamaguchi[19] considered 306 atoms in 7 layers, 12 in the first layer and 49 in each of the lower 6 layers. This model gives a strain energy equal to 77.4 eV per unit cell for the unrelaxed structure. In contrast, the same model of the Binnig structure with the same lattice potential gives a strain energy of 86.0 eV per unit cell for the unrelaxed structure if the atoms in layer B are allowed to interact with a sufficient number of atoms in layer C to form three bonds with each layer B atom. This increase in the strain energy of 8.6 eV/unit cell is due to six extra three-body terms present in the model shown in Fig. 1 but not in the model treated by Yamaguchi.[19] If these terms are omitted, a strain energy of 77.4 eV/unit cell is obtained.

A number of lattice potentials suitable for the silicon system are now available.[33,34] The simplest among these is that given by Keating,[33] for which

$$V_L = \sum_{i,j} (f_a/2)\,[\mathbf{r}_{ij}\cdot\mathbf{r}_{ij} - \mathbf{R}_{ij}\cdot\mathbf{R}_{ij}]^2/[\mathbf{R}_{ij}\cdot\mathbf{R}_{ij}]$$

$$- \sum_{i,j,k} (f_b/8)\,[\mathbf{r}_{ij}\cdot\mathbf{r}_{ik} - \mathbf{R}_{ij}\cdot\mathbf{R}_{ik}]^2/[\mathbf{R}_{ij}\cdot\mathbf{R}_{ik}], \qquad (1)$$

where for Si, $\mathbf{R}_{ij}\cdot\mathbf{R}_{ik} = -6.581$ a.u.^{2}, $\mathbf{R}_{ij}\cdot\mathbf{R}_{ij} = 19.74$ a.u.^{2}, and $\mathbf{r}_{ij}$ is the vector between lattice atoms i and j. The bond-stretching and bond-bending force constants, f_a and f_b, sug-

gested by Keating for the unreconstructed surface are 0.636 and 0.483 eV/a.u.^{2}, respectively.[33]

For the (7×7) reconstructed surface model suggested by Binnig *et al.*,[17] there are, per unit cell, 36 angles between vectors $\mathbf{r}_{ij}$ and $\mathbf{r}_{ik}$ that have a value of 180° and 24 angles that have a value of 70.53°. If the parameter value suggested by Keating for f_b is used for the reconstructed surface, the contribution to the strain energy by the three-body bending term in Eq. (1) for each of these 60 angles is 2.86 eV. This yields a total strain energy of 171.6 eV, which is over twice the value given by Yamaguchi[19] for 54 such terms. Although Yamaguchi did not specify the value of f_b used in his calculations, it would appear that he employed a value half that suggested by Keating. Other considerations show that such a reduction is appropriate for the (7×7) surface.

If we assume that in the $(1\times1)\rightarrow(7\times7)$ reconstruction 49 dangling bonds are reduced to 25 dangling bonds per unit cell, then it can be shown that during reconstruction the equivalent of 12 new bonds/(7×7) unit cell are formed. Consider n (7×7) unit cells each having N atoms. In the (1×1) phase, there would be $49n$ atoms having dangling bonds, i. e., $49n$ atoms would have three bonds each and $nN-49n$ atoms would have four bonds each. Since one bond is shared by two atoms, there would be $0.5[4\times(nN-49n)+3\times49n]$ bonds. Similarly, there would be $0.5[4\times(nN-25n)+3\times25n]$ bonds in the (7×7) reconstruction. Therefore, the increase in the number of Si–Si bonds due to the $(1\times1)\rightarrow(7\times7)$ transition is

$$0.5\{[4\times(nN-25n)+3\times25n] - [4\times(nN-49n)+3\times49n]\} = 12n. \quad (2)$$

For the reconstruction to occur, it is necessary that the energy released by the formation of these 12 bonds be greater than the strain energy produced by the reconstruction. It is known[34(a)] that the energy released per bond is about 2.1 eV which amounts to 25.2 eV per (7×7) unit cell. With $f_b = 0.483$ eV/a.u.^{2}, the corresponding strain energy is 171.6 eV for the unrelaxed structure. This energy is reduced to 141.1 eV if we allow the lattice to relax, but this is still much too large to permit reconstrution.

Since the reconstruction to a (7×7) structure is known to occur spontaneously, the above analysis shows that a bending force constant of 0.483 eV/a.u.^{2} is too large. This is not surprising since the Keating potential parameter has been fitted for the near equilibrium tetrahedral geometry.

In contrast, if we employ the lattice potential suggested by Brenner and Garrison[34(a)] for both the reconstructed and (1×1) silicon surfaces, the strain energy of the unrelaxed surface per (7×7) unit cell is 5. 0 eV less than the energy released in the formation of 12 bonds, which seems reasonable. While we could use the Brenner–Garrison potential in the study of heterogeneous SiH_2 surface reactions, the significantly greater complexity of this potential would require a much greater investment of computational time. Since the computational requirements are already very large, we have elected to use the Keating lattice potential[33] with f_b adjusted to give the same strain energy as that obtained with the Brenner–Garrison potential.[34(a)] This criterion gives $f_b = 0.0514$ eV/a.u.^{2}.

The relaxation studies of the silicon lattice using the Keating potential with this lower value of f_b shows that the geometry of the Binnig *et al.*[17] 7×7 reconstruction is maintained. The RMS change in bond length for all 693 bonds of the model lattice is 2.2%. The maximum percent change in bond lengths are 2.2%, 3.8%, and 10.4% for bonds between the successive layers of the lattice. The relatively large value for bonds between the third and fourth layers is due to the fact that, in the present model, the positions of the fourth layer atoms are fixed. The use of a larger lattice model would be expected to reduce this value.

III. POTENTIAL ENERGY SURFACE

The potential-energy surface used for the SiH_2–Si(111)–(7×7) system is that employed in I for the SiH_2–Si(111)–(1×1) system. This potential is written as the separable sum of a lattice potential V_L, a gas–lattice interaction term V_{gL}, and a SiH_2 intramolecular potential V_g:

$$V = V_L + V_{gL} + V_g. \quad (3)$$

Except for the modifications described below, each of these terms is identical to the corresponding term in I.

The lattice potential V_L is the Keating potential,[33] Eq. (1), as used in I. The bending parameter f_b, however, has been adjusted to give a lattice strain energy equal to that obtained from the Brenner–Garrison[34a] surface. This adjustment gives $f_b = 0.0514$ eV/a.u.^{2}.

With respect to the gas–lattice interaction term V_{gL}, all atoms with dangling bonds in the (7×7) reconstruction are treated as described in I for first-layer atoms. The treatment of the remaining 253 atoms is as described for second-layer atoms in I.

In I, the silicon atom in SiH_2, Si(g), is assumed to interact only with the central 9 atoms of the first layer and with 16 atoms of the second layer. For the (7×7) reconstruction, we allow the summation of Si(g)–lattice interactions to run over all atoms of the model lattice. The attenuation function $S^{(2)}(i)$ occurring in Eq. (19) of I is taken to be unity for the (7×7) surface since the geometry of the reconstruction does not permit Si(g) to form simultaneous Si–Si bonds with more than one lattice atom.

In I, the interaction between the ith lower-layer lattice atom and Si(g), denoted by $V^{II}_{Si}(3,i)$, was taken to have an inverse R^{12} form with arbitrarily assigned parameter values. In the present study, we have obtained a more accurate estimate of this repulsive potential from the results of SCF(3-21G) calculations on the Si–SiH_4 system. Figure 2 shows the SCF results as a function of the Si–Si distance along a C_2 symmetry axis. Nonlinear, least-squares fitting of these data to an exponential function gives

$$V^{II}_{Si}(3,i) = 1119.13\exp[-1.427R_{3i}]\ \text{eV}, \quad (4)$$

where R_{3i} is the distance between Si(g) and the ith lattice atom in a.u. Equation (4) is used in place of the arbitrary R^{-12} function employed in I.

The factor $V^I_M(k,i)$, which appears in Eqs. (14) and (16) of I, gives the interaction between the k th ($k = 1,2$) hydrogen atom and the ith lattice atom. The use of this functional form in I gave a Si–Si–H bending frequency that was

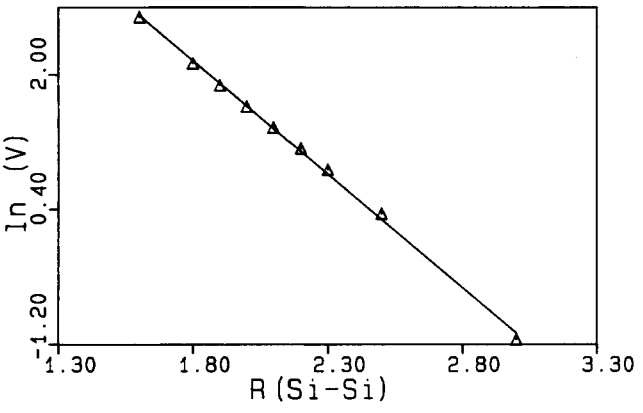

FIG. 2. Variation of the Si–SiH_4 potential computed from SCF calculations with a 3-21G basis set. The abscissa gives the Si–Si distance along a C_2 axis. The solid line is a nonlinear least-squares fit of Eq. (3) to the data.

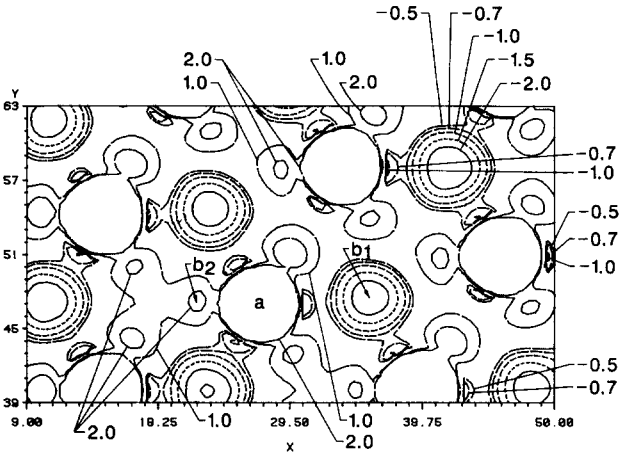

FIG. 4. Contour plot for the interaction potential V between Si(g) and the relaxed (7×7) lattice as a function of X and Y in a plane parallel to and 4.0 a.u. above atom b_1 of the second layer as shown in Fig. 1. X and Y are in a.u. and V is in eV. The points marked a, b_1, and b_2 refer to the X–Y coordinates of the corresponding points marked in Fig. 1.

too small. In the present work, we have therefore replaced $V_M^I(k,\mathrm{i})$ with $V_M^I(k,\mathrm{i},\theta)$ where

$$V_M^I(k,i,\theta) = V_M^I(k,i)[1 + a_1\cos\theta + a_2\cos^2\theta]/[1 + a_1 + a_2] \quad (5)$$

with θ being the angle between the surface normal and the i–k vector. The parameters a_1 and a_2 are used to adjust the Si–Si–H bending frequency. With $a_1 = 1.0$ and $a_2 = 4.0$, a power spectrum of the hydrogen atom–surface motion gives a bending frequency of 621 cm^{-1} with a resolution of 5.4 cm^{-1}. This result is in good accord with the available experimental data which lie in the range 630–637 cm^{-1}.[9,35,36] The surface–hydrogen stretching frequency obtained with Eq. (5) is 2089 cm^{-1}, which is also in close agreement with the experimental values that range from 2057 to 2100 cm^{-1}.[9,35–37]

Figures 3–6 depict various features of the potential-energy surface. Figures 3 and 4 describe the interaction potential between the relaxed (7×7) lattice and a Si(g) atom placed in a plane parallel to the surface at a height of 4.0 a.u. from the lattice atoms a and b_1 (see Fig. 1), respectively. Atom a lies in layer A while b_1 is a B-layer atom with a dangling bond. Figures 5 and 6 show the equivalent potentials for a hydrogen atom in a plane 3.0 a.u. above lattice atoms a and b_1, respectively.

The deep potential wells seen in Figs. 3 and 5 immediately above the location of the first-layer adatoms are due to the formation of *–Si and *–H bonds, respectively. At this height, the effect of all surface atoms other than those in layer A is too small to be seen on the potential scales used in these figures. The contour plots given in Figs. 4 and 6 show the potential wells above the layer B atoms with dangling bonds, e. g., location b_1. The effect of the repulsive interactions with the closed-shell lattice atoms in layer B is shown by the point marked b_2 in Fig. 4. This point corresponds to that so marked in Fig. 1. The corresponding repulsive wall at point b_2 is absent in Fig. 6 due to the fact that the H–Si repulsive interaction is not as large as that for Si–Si.

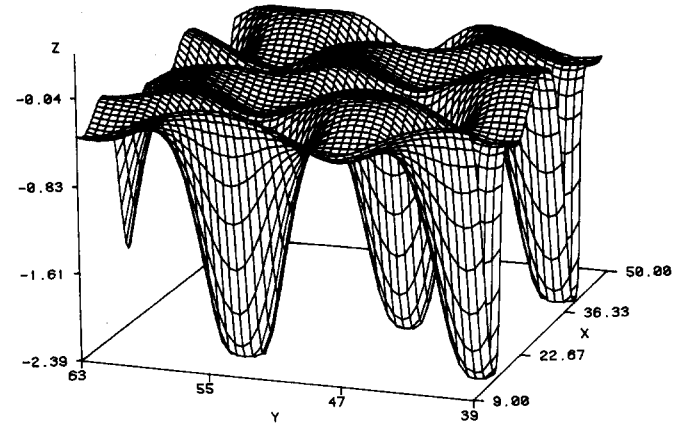

FIG. 3. The interaction potential V (z axis) in eV between Si(g) and the relaxed (7×7) lattice as a function of X and Y in a.u. in a plane parallel to and 4.0 a.u. above atom a of the top layer of the Si(111)–(7×7) lattice as shown in Fig. 1.

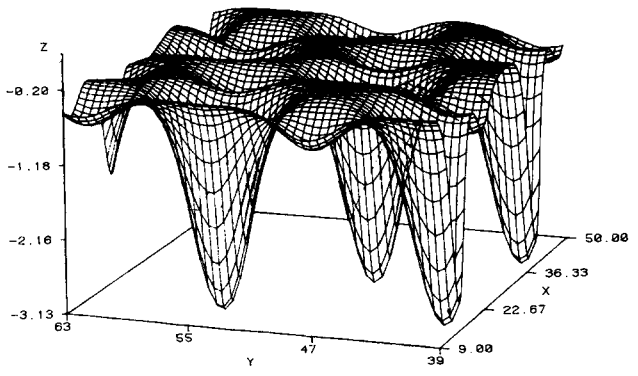

FIG. 5. The interaction potential V (z axis) in eV between H and the relaxed (7×7) lattice as a function of X and Y in a.u. in a plane parallel to and 3.0 a.u. above atom a of the top layer of the Si(111)–(7×7) lattice as shown in Fig. 1.

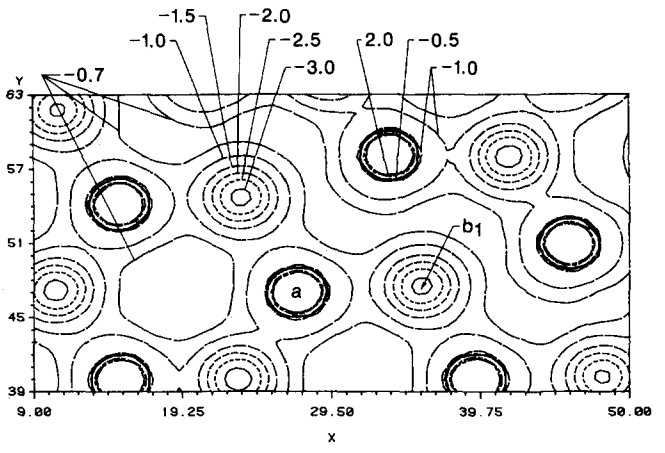

FIG. 6. Contour plot for the interaction potential V between H and the relaxed (7×7) lattice as a function of X and Y in a plane parallel to and 3.0 a.u. above atom b_1 of the second layer as shown in Fig. 1. X and Y are in a.u. and V is in eV. The points marked a, b_1, and b_2 refer to the X–Y coordinates of the corresponding points marked in Fig. 1.

IV. RESULTS

A. Methods

The dynamics of the SiH_2–Si(111)–(7×7) system are investigated using standard trajectory methods.[38] Metropolis sampling procedures[39] are employed to average over the initial phase space of the lattice. The parameters for the Markov random walk and the numerical integration procedure are the same as described in I. The integration step size is 3.77×10^{-16} s, which we define to be one time unit (t.u.). With one exception, trajectories are integrated up to a maximum period of 10 000 steps. The selection of initial positions and momenta for SiH_2 incident on Si(111)–(1×1) is identical to that used in I. In this case, the aiming points are always taken as the central portion of the model lattice since all lattice points on the (1×1) surface are equivalent. For the (7×7) surface, such symmetry is absent. We therefore select aiming points randomly from a flat distribution over the entire unit cell. The unit cell is shown as the area inside the parallelogram of Fig. 1. The direction of the incident SiH_2 velocity vector is determined by a random choice of the rotation angle ϕ from a uniform distribution over the range [0°, 180°] and by the random selection of the azimuthal angle θ over the range [0°,90°] from a distribution weighted by sin θ. The initial perpendicular distance from Si(g) to the surface plane is taken to be 10.0 a.u. At a height of 7.5 a.u., the magnitude of the interaction term V_{gL} is less than 0.1 eV.

Since our lattice model is of limited size, it is not possible to study the effect of gas–lattice collisions that occur at θ angles near 90°. The trajectories of such collisions would be significantly influenced by surface atoms far outside the unit cell shown in Fig. 1. Since these lattice atoms are absent in the present model, these processes cannot be accurately investigated. To avoid the inclusion of such trajectories, we require that an undeviated SiH_2 trajectory be such that at a height of 7.5 a.u. above the surface plane, the (x,y) coordinates of Si(g) lie within the region bounded by the 81 atoms of the second layer of the (7×7) lattice. If this condition is not satisfied, the initial conditions for θ and ϕ for that trajectory are discarded and new values are selected until an acceptable trajectory is obtained.

In all calculations, the initial SiH_2 translational energy is 0.1034 eV. The initial SiH_2 vibrational and rotational energies are zero. The lattice temperature is taken to be 1000 K. The large CPU time required to calculate the trajectories has limited the study to a total of 150 trajectories for the (7×7) lattice and 100 trajectories for (1×1) surface.

B. Observed reactions

The primary step in the process is either the scattering or chemisorption of SiH_2. Two chemisorption channels are open. That is, we expect either

$$* + SiH_2 \rightarrow * + SiH_2(\text{scattering}), \quad \text{(R1)}$$

$$* + SiH_2 \rightarrow *\text{--}SiH_2, \quad \text{(R2)}$$

or

$$2* + SiH_2 \rightarrow *\text{--}SiH_2\text{--}*. \quad \text{(R3)}$$

Reaction (R2) represents SiH_2 chemisorbtion to a single, on-top site. Reaction (R3) denotes the formation of two tetrahedral Si–Si bonds between two adjacent sites. For the (1×1) surface, every trajectory examined in this study and in I resulted in reaction (R3). Thus, the sticking probability is either unity or very close to unity. For the (7×7) surface, the result is very different. The relative positions of atoms with dangling bonds on this reconstruction are such that the formation of two tetrahedral bonds is not energetically possible. Reaction (R3) is therefore never observed. Five of the 150 trajectories investigated resulted in scattering from Si(111)–(7×7). We therefore estimate the sticking probability on this surface modification to be about 0.97.

Since the exothermicity of reaction (R3) is almost twice that for reaction (R2), the energy available for further reactions of the chemisorbed SiH_2 is significantly more for reaction on the (1×1) surface than on Si(111)–(7×7). This consideration, coupled with the very different geometries of the two surfaces, suggests that the decomposition pathways will be very different.

The direct elimination of molecular H_2 subsequent to SiH_2 chemisorption has been observed for both surfaces. For the (7×7) reconstruction, 17 trajectories out of 145 resulted in

$$*\text{--}SiH_2 \rightarrow *\text{--}Si + H_2\,(\text{gas}). \quad \text{(R4)}$$

For the (1×1) surface, 20 trajectories out of 100 decomposed via

$$*\text{--}SiH_2\text{--}* \rightarrow *Si\text{--}* + H_2(\text{gas}). \quad \text{(R5)}$$

Decomposition of SiH_2 via dissociation of hydrogen atoms to adjacent surface binding sites was found in I to be the major reaction pathway for chemisorbed SiH_2. This reaction,

$$*\text{--}SiH_2\text{--}* + * \rightarrow *\text{--}SiH\text{--}* + *\text{--}H, \quad \text{(R6)}$$

is still found to be an important decomposition pathway on Si(111)–(1×1) with the modified potential surface described above. Reaction into this channel was observed in 16 of the 100 trajectories examined on the (1×1) surface. The

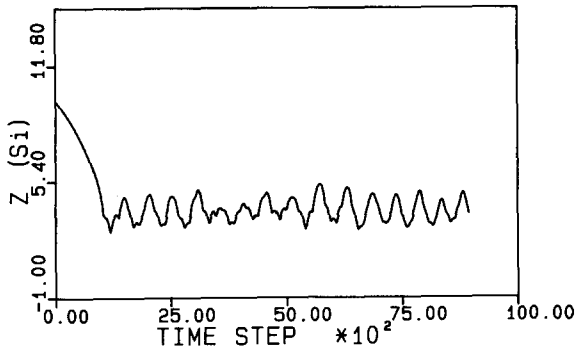

FIG. 7. Perpendicular distance in a.u. of Si(g) from the Si(111)-(7×7) surface plane as a function of time in trajectory number 1. One time step = 3.77×10^{-16} s.

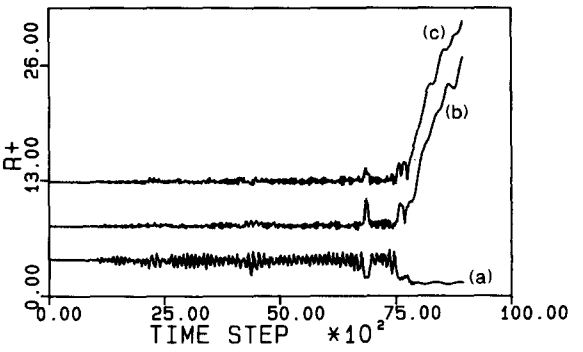

FIG. 9. Variation of Si–H and H–H distances for trajectory number 1: One time step = 3.77×10^{-16} s. (a) R + = H–H distance in a.u. (b) R + = 5.0 + distance between Si(g) and H number 1. (c) R + = 10.0 + distance between Si(g) and H number 2.

corresponding reaction on the (7×7) recontructed surface,

$$*\text{--}SiH_2 + * \rightarrow *\text{--}SiH + *\text{--}H, \qquad (R7)$$

was never observed as a final reaction product. Reaction (R7) was observed to occur in four trajectories at times between 5000–9000 steps, however, the products were very short-lived with the reverse reaction,

$$*\text{--}SiH + *\text{--}H \rightarrow *\text{--}SiH_2 + *, \qquad (R8)$$

taking place to reform the original chemisorbed SiH_2 molecule. The lifetimes of the products of reaction (R7) varied from $(1.13\text{–}10.6)\times10^{-13}$ s.

Figures 7–15 illustrate typical mechanistic features of the decomposition reactions on Si(111)-(7×7). Figures 7–10 show the details of a trajectory (#1) leading to molecular elimination of H_2. The variation of the z coordinate of Si(g) with time is given in Fig. 7. This coordinate is in the direction of the surface normal with $z = 0$ corresponding to the surface plane. Figure 8(a) gives the sum of the kinetic and interaction potential energies for Si(g) as a function of time. At $t = 0$, Si(g) is far from the surface and this sum is equal to the initial kinetic energy, 0.1034 eV. Both Figs. 7 and 8 show that chemisorption, reaction (R2), occurs at $t = 1100$ t.u. for this particular trajectory. The exothermicity of this reaction is partially released into the Si–H bonds as well as into the phonon modes of the lattice. Curve B in Fig. 8 gives the time variation of the sum of the kinetic energies of the two hydrogen atoms, the SiH_2 intramolecular potential relative to that for the gas-phase equilibrium structure, and the potential energy of the two hydrogen atoms due to interaction with the lattice. Curve C gives the sum of the kinetic and potential energy of the lattice atoms. These results show that after some of the exothermicity is released to the lattice upon impact and chemisorption, further energy dissipation to the lattice modes either does not occur or is a slow process.

Figure 9 shows the time variation of the three interatomic distances for the incident SiH_2 molecule. The large amplitude oscillations of the H–H distance compared to the corresponding Si–H distances indicates that upon chemisorption, most of the internal SiH_2 energy is contained in the bending mode. The Si–H stretching modes are gradually excited until at $t = 7500$ t.u. there is a concerted rupture of the two Si–H bonds forming H_2. Figure 10, which gives the time dependence of the z coordinate of one of the hydrogen atoms, shows that the molecular hydrogen formed at 7500 t.u. is released directly into the gas phase.

Figures 11–15 show analogous results for a second trajectory leading to reactions (R2), (R7), and (R8). Figures

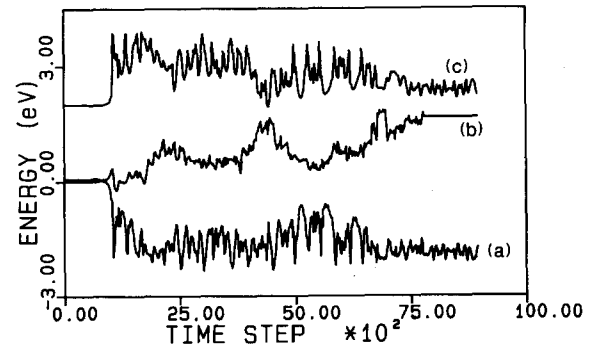

FIG. 8. Energy transfer in trajectory number 1: One time step = 3.77×10^{-16} s. (a) kinetic energy of Si(g) + interaction energy of this atom with the lattice relative to the potential with Si(g) at an infinite distance; (b) kinetic energy of two hydrogen atoms + potential of SiH_2 relative to its equilibrium value + interaction potential of hydrogen atoms with the lattice relative to that with hydrogens at infinite distance; (c) kinetic- + potential energy of the silicon lattice + 2. 0 eV. The initial potential- + kinetic energy is taken as zero.

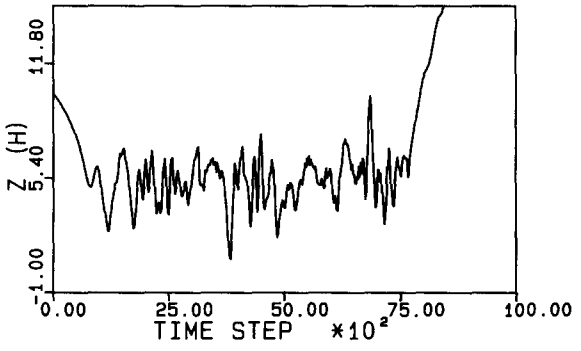

FIG. 10. Perpendicular distance in a.u. of H from the Si(111)-(7×7) surface plane as a function of time in trajectory number 1. One time step = 3.77×10^{-16} s.

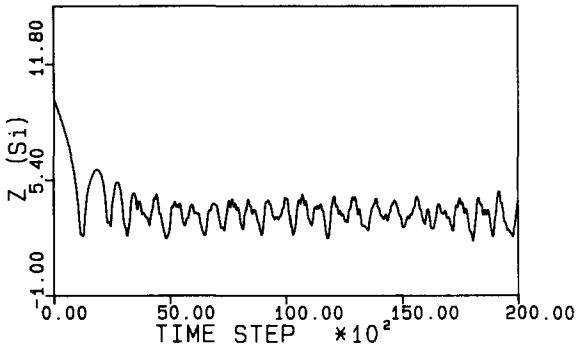

FIG. 11. Perpendicular distance in a.u. of Si(g) from the Si(111)–(7×7) surface plane as a function of time in trajectory number 2. One time step = 3.77×10^{-16} s.

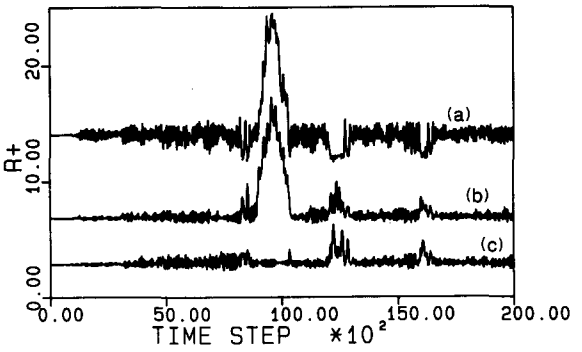

FIG. 13. Variation of Si–H and H–H distances in a.u. for trajectory number 2. One time step = 3.77×10^{-16} s. (a) R + = H–H distance + 10.0. (b) R + = distance between Si(g) and H number 1 + 4.0. (c) R + = distance between Si(g) and H number 2.

11 and 12(a) show chemisorption occurring at 1000 t.u. The larger vibrational amplitude of Si(g) with the surface seen in Fig. 11 compared to that of Fig. 7 shows that in this trajectory more of the energy initially resides in the *–Si stretching mode. As a consequence, less energy is dissipated in the lattice modes upon chemisorption. The total lattice energy is seen to remain almost constant up to $t = 12{,}000$ t. u. Figure 12 shows that this *–Si stretching energy is gradually transferred into SiH_2 internal motions involving the hydrogen atoms causing reaction (R7) at $t = 9000$ t.u.

The relatively rare occurrance of reaction (R7) is seen in Figs. 13–15 around 9000 t.u. The z coordinate of Si(g) upon chemisorption in this trajectory indicates that SiH_2 is bound to a silicon atom in layer A. In Fig. 13, one Si–H and the H–H distances increase to that characteristic of a hydrogen atom bonded to the nearest layer B atom with a dangling bond. The z coordinate of the dissociated hydrogen atom given in Fig. 14 is that expected for chemisorption to a layer B site. The time variation of the (x,y) coordinates (not shown) confirms this point. Figures 13-15 all show reaction (R8) occurring at 10 400 t.u. The lifetime of the chemisorbed hydrogen atom in this trajectory is therefore about 5.28×10^{-13} s.

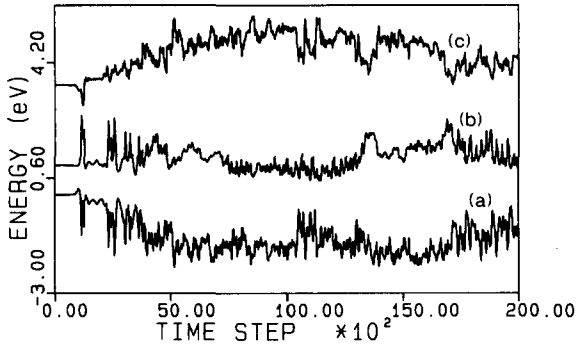

FIG. 12. Energy transfer in trajectory number 2: One time step = 3.77×10^{-16} s. (a) Kinetic energy of Si(g) + interaction energy of Si(g) with the lattice relative to that with Si(g) at an infinite distance; (b) kinetic + potential energy of the silicon lattice + 1.0 eV. The initial potential + kinetic energy is taken to be zero; (c) kinetic energy of two hydrogen atoms + potential energy of SiH_2 relative to its equilibrium value + interaction energy of hydrogen atoms with the lattice relative to that when hydrogen atoms are at infinity + 3.5 eV.

C. Rate coefficients

We have extracted estimates of the rate coefficients for each of the important decomposition modes on Si(111)–(7×7) and Si(111)–(1×1) assuming that each process may be described by first-order kinetics. Under this assump-

$$\frac{dA}{dt} = -(k_5 + k_6)\mathrm{A} \tag{6}$$

and

$$k_5/k_6 = (B/C) \text{ at } t = \infty, \tag{7}$$

where A, B, and C denote the concentrations of *--SiH_2--*, H_2, and *--SiH--*, respectively. If we assume that the final B/C ratio is that present at 10 000 t.u., we obtain $k_5 = 6.6\times10^{10}$ and $k_6 = 5.3\times10^{10}$ s^{-1}.

Using similar assumptions, the rate coefficients k_4 and k_7 for reactions (R4) and (R7), are found to be 3.4×10^{10} and 0.79×10^{10} s^{-1}, respectively. In less than 2800 t.u., all trajectories in which reaction (R7) has occurred subsequently undergo reaction (R8). We may obtain an estimate of the order of magnitude of k_8 from

$$k_8 = [\ln(4/1)]/t_0, \tag{8}$$

where t_0 is the time required for three of the four trajectories to react via (R8). This yields $k_8 = 1.4\times10^{12}$ s^{-1}, which suggests that the recombination reaction (R8) is about 180

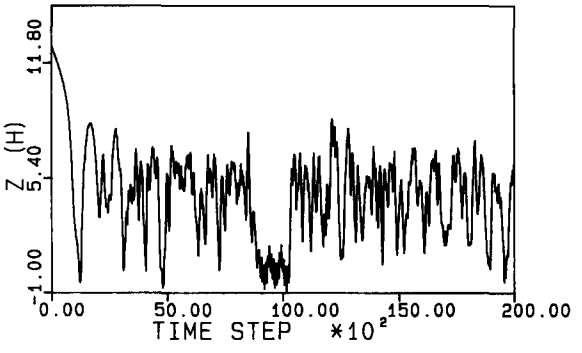

FIG. 14. Perpendicular distance in a.u. of the dissociating H atom from the Si(111)–(7×7) surface plane as a function of time in trajectory number 2. One time step = 3.77×10^{-16} s.

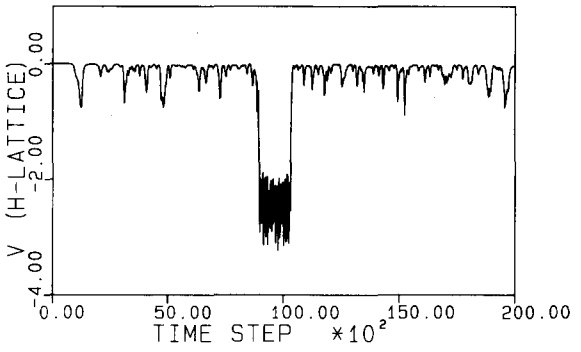

FIG. 15. The interaction energy in eV between the lattice and the dissociated hydrogen atom in trajectory number 2. The zero of potential corresponds to the hydrogen atom at an infinite distance from the lattice. One time step = 3.77×10^{-16} s.

times faster than decomposition processes leading to hydrogen atom dissociation to adjacent lattice sites. It is therefore not surprising that the reaction

$$*\text{--SiH} + * \rightarrow *\text{--Si} + *\text{--H} \qquad \text{(R9)}$$

is not observed.

The results for all rate coefficients are summarized in Table I.

D. Discussion

The modulated molecular beam experiments reported by Farnaam and Olander[5] show that simultaneous surface reactions of SiH_4 and SiD_4 lead only to the production of H_2 and D_2. The fact that no HD is observed indicates that the reaction mechanism does not involve the production of chemisorbed hydrogen atoms. The present calculations predict that while the production of *--H is an important decomposition reaction on the (1×1) surface, it is a slow process on the (7×7) reconstructed surface. The results also show that the expected lifetime of the *--H species is very short. Nevertheless, the transient production of chemisorbed hydrogen atoms indicates that in a mixed experiment involving the simultaneous deposition of SiH_2 and SiD_2, we would expect the formation of some *--SiHD and *--SiDH which eventually would lead to the formation of HD(g) via reaction (R4).

The apparent disagreement between the experimental results[5] and the present calculations are probably due to energetic differences in the surface decomposition of SiH_4 and SiH_2. In the former case, some energy must be expended to break one of the Si–Si bonds of the lattice to form the divalent silicon atom needed for the initial formation of two SiH_2 molecules on the surface as proposed by Farnaam and Olander.[5] This reaction,

$$SiH_4 + * + *\text{--}* \rightarrow *\text{--}SiH_2 + H\text{--}*\text{--}H + *, \qquad \text{(R10)}$$

is probably nearly thermochemically neutral. If so, then the *--SiH_2 formed in SiH_4 deposition will have very little internal energy content. In contrast, direct chemisorption of SiH_2 leads to highly excited *--SiH_2. The reaction rates in this case would therefore be expected to be significantly larger. This view is supported by the fact that Farnaam and Olander[5] report (R4) reaction rates of 5.9×10^2 s^{-1} or less at a surface temperature of 1000 K. We may estimate the corresponding thermal result for our model system using the barrier height for reaction (R4) given by our potential as the activation energy. If we assume that the rate coefficients given in Table I represent the high-temperature limiting values, we obtain an extrapolated thermal rate of 9.4×10^2 s^{-1} at 1000 K which is in fair accord with the Farnaam and Olander[5] results.

The rate coefficients obtained for reactions (R5) and (R6) in the present study are significantly less than the corresponding rate coefficients obtained in paper I. Furthermore, the reaction

$$*\text{--SiH--}* + * \rightarrow *\text{--Si--}* + *\text{--H} \qquad \text{(R11)}$$

for which we obtained $k_{11} = 1.7\times10^{12}$ s^{-1} in I, was not observed in the present calculations. These differences are due to the changes in the interaction potential introduced by Eqs. (3) and (4). Equation (4) is introduced to obtain a more accurate bending frequency for the *--H bond which was near zero in I. With this bending frequency adjusted to 621 cm^{-1} a *--H bond normal to the surface plane is energetically favored. This change increases the barrier for the hydrogen–atom dissociation reactions, (R6) and (R11), and thereby significantly reduces the calculated rates for these reactions.

Equation (3) modifies the repulsive interaction of Si (g) with the lattice atoms without dangling bonds with the result that the repulsive potential experienced by Si(g) in *--SiH_2--* is increased. This modification reduces the exothermicity for the chemisorption process (R3) which reduces the reaction rates. Since the present *--H bending frequency is known to be in accord with experiment[9,35,36] and the repulsive interaction has been obtained from *ab initio* SCF calculations rather than taken arbitrarily, we expect the present results to be a better estimate of the true rates than those previously reported.[3]

If the studies were carried out on the DAS model[20,21] of the (7×7) reconstructed surface, we might expect a smaller sticking coefficient since the number of dangling bonds per

TABLE I. Rate coefficients and sticking probabilities for SiH_2 deposition/decomposition reactions on Si(111)–(1×1) and Si(111)–(7×7) surfaces. Error limits represent one sigma limit of statistical uncertainty.

Reaction	N^a	$k\times10^{10}$ s^{-1}
Si(111)–(1×1)		
Total number of trajectories = 100		
$2* + SiH_2 \rightarrow *\text{–}SiH_2\text{–}*$	100	...
$*\text{–}SiH_2\text{–}* + * \rightarrow *\text{–}SiH\text{–}* + *\text{–}H$	16	5.3 ± 1.2
$*\text{–}SiH_2\text{–}* \rightarrow *\text{–}Si\text{–}* + H_2$	20	6.6 ± 1.3
Si(111)–(7×7)		
Total number of trajectories = 150		
$* + SiH_2 \rightarrow *\text{–}SiH_2$	145	...
$*\text{–}SiH_2 + * \rightarrow *\text{–}SiH_2\text{–}*$	0	0
$*\text{–}SiH_2 + * \rightarrow *\text{–}SiH + *\text{–}H$	4	0.79 ± 0.4
$*\text{–}SiH_2 \rightarrow *\text{–}Si + H_2$	17	3.4 ± 0.8

[a] Number of trajectories undergoing reaction.

unit surface area is less for the DAS than for the Binnig surface. We would expect the rate coefficient for reaction (R4) to be almost the same for both of these models. However, k_7 may decrease on the DAS surface since there are fewer favorable neighboring pairs that have dangling bonds. These points are currently under study.

ACKNOWLEDGMENTS

We are pleased to acknowledge financial support from the Air Force Office of Scientific Research under Grant AFOSR-89-0085. Some of the calculations reported in this paper were carried out on a VAX 11/780 purchased, in part, with funds provided by grants from the Department of Defense University Instrumentation Program, AFOSR-85-0115, and the Air Force Office of Scientific Research, AFOSR-86-0043. P.M.A expresses his thanks to Vikram University, Ujjain, India, for granting him leave to pursue this research.

[1]J. M. Jasinski, B. S. Meyerson, and B. A. Scott, Annu. Rev. Phys. Chem. **38**, 109 (1987).
[2]J. Bloem and L. J. Giling, *Current Topics in Material Science*, edited by E. Kaldis (North-Holland, Amsterdam, 1978), Chap. 4.
[3]P. M. Agrawal, D. L. Thompson, and L. M. Raff, Surf. Sci. **195**, 283 (1988).
[4]R. Robertson and A. Gallagher, J. Chem. Phys. **85**, 3623 (1986).
[5]M. K. Farnaam and D. R. Olander, Surf. Sci. **145**, 390 (1984).
[6]For a review, see D. Haneman, Rep. Prog. Phys. **50**, 1045 (1987).
[7]B. G. Koehler, C. H. Mak, D. A. Arthur, P. A. Coon, and S. M. George, J. Chem. Phys. **89**, 1709 (1988).
[8](a) C. M. Greenlief, S. M. Gates, and P. A. Holbert, J. Vac. Sci. Technol. (to be published), (b) S. M. Gates, Surf. Sci. **195**, 307 (1988).
[9]M. Nishijima, K. Edamoto, Y. Kubota, H. Kobayashi, and M. Onchi, Surf. Sci. **158**, 422 (1985).
[10]M. Wautelet, Surf. Sci. **187**, L655 (1987).
[11]D. A. Outka, J. Stohr, R. J. Madix, H. H. Rotermund, B. Hermsmeier, and J. Solomon, Surf. Sci. **185**, 53 (1987).
[12]G. Akinci, T. R. Ohno, and E. D. Williams, Surf. Sci. **193**, 534 (1988).
[13]I. Ichikawa, Surf. Sci. **136**, 267 (1984).
[14]K. Edamoto, S. Tanaka, M. Onchi, and M. Nishijima, Surf. Sci. **167**, 285 (1986).
[15]M. Nishijima, H. Kobayashi, K. Edamoto, and M. Onchi, Surf. Sci. **137**, 473 (1984).
[16]P. Funke and G. Materlik, Surf. Sci. **188**, 378 (1987).
[17](a) G. Binnig, H. Rohrer, Ch. Gerber, and E. Weibel, Phys. Rev. Lett. **50**, 120 (1983); (b) G. Binnig, H. Rohrer, F. Salvan, Ch. Gerber, and A. Baro, Surf. Sci. **157**, L373 (1985).
[18]R. M. Tromp, Surf. Sci. **155**, 432 (1985).
[19]T. Yamaguchi, Phys. Rev. B **30**, 1992 (1984).
[20]K. Takayanagi, Y. Tanishiro, S. Takahashi, and M. Takahashi, Surf. Sci. **164**, 367 (1985).
[21]K. Takayanagi, Y. Tanishiro, M. Takahashi, and S. Takahashi, J. Vac. Sci. Technol. A **3**, 1502 (1985).
[22]D. J. Chadi, R. S. Bauer, R. H. Williams, G. V. Hansson, R. Z. Bachrach, J. C. Mikkelsen, F. Houzay, G. M. Guichar, R. Pinchaux, and Y. Petroff, Phys. Rev. Lett. **44**, 799 (1980).
[23]D. J. Miller, D. Hanaman, and L. W. Walker, Surf. Sci. **94**, 555 (1980).
[24]D. J. Miller and D. Haneman, Surf. Sci. **104**, L237 (1981).
[25]W. A. Harrison, Surf. Sci. **55** 1 (1976).
[26]M. Aono, R. Souda, C. Oshima, and Y. Ishizawa, Phys. Rev. Lett. **51**, 801 (1983).
[27]L. C. Synder, Surf. Sci. **140**, 101 (1984).
[28]P. A. Bennett, L. C. Feldman, Y. Kuk, E. G. McRae, and J. E. Rowe, Phys. Rev. B **28**, 3656 (1983).
[29]E. G. McRae, Phys. Rev. B **28**, 2305 (1983).
[30]F. J. Himpsel, Phys. Rev. B **27**, 7782 (1983).
[31]F. J. Himpsel and I. Batra, J. Vac. Sci. Technol. A **2**, 952 (1984).
[32]R. M. Tromp and E. J. van Loenen, Surf. Sci. **155**, 441 (1985).
[33]P. N. Keating, Phys. Rev. **145**, 637 (1966).
[34](a) D. W. Brenner and B. J. Garrison, Phys. Rev. B **34**, 1304 (1986); (b) B. W. Dodson, *ibid.* **35**, 2795 (1987); (c) J. Tersoff, Phys. Rev. Lett. **56**, 632 (1986); (d) R. Biswas and D. R. Hamann, *ibid.* **55**, 2001 (1985); (e) F. H. Stillinger and T. A. Weber, Phys. Rev. B **31**, 5262 (1985); (f) E. Pearson, T. Takai, T. Halicioglu, and W. A. Tiller, J. Crystal Growth **70**, 33 (1984).
[35]H. Wagner, R. Butz, U. Backes, and D. Bruchmann, Solid State Commun. **38**, 1155 (1981).
[36]H. Kobayashi, K. Edamoto, M. Onchi, and M. Nishijima, J. Chem. Phys. **78**, 7429 (1983).
[37]H. Froitzheim, U. Kohler, and H. Lammering, Surf. Sci. **149**, 537 (1985).
[38]L. M. Raff and D. L. Thompson, *Classical Trajectory Approach to Reactive Scattering*, in *Theory of Chemical Reaction Dynamics*, edited by M. Baer (CRC, Boca Raton, FL, 1985), Vol. III, p. 1.
[39]N. Metropolis, A. W. Rosenbluth, M. Rosenbluth, A. H. Teller, and E. Teller, J. Chem. Phys. **21**, 1087 (1953).